

Application of GaAs Device Technology to Millimeter-Waves

Tsuneo TOKUMITSU*, Miki KUBOTA, Kazuo SAKAI and Takahisa KAWAI

This paper introduces a novel three-dimensional wafer-level chip size package (3-D WLCSP) technology developed by Sumitomo Electric Device Innovations, Inc. and Sumitomo Electric Industries, Ltd. Our 3-D WLCSP monolithic microwave integrated circuit (MMIC) employs 0.1 μm -gate AlGaAs/GaAs pseudomorphic high electron mobility transistors (PHEMTs) and is designed to be flip-chip assembled as an excellent platform at all frequencies from 10 GHz to millimeter-waves. In the millimeter-wave region, the 76 GHz- and 79 GHz-bands automotive radars are rapidly growing in popularity and the 80 GHz-band (E-band) high-speed microwave communication transceiver is taking off in production. This paper describes our 3-D WLCSP MMIC for such applications, making a comparison between 3-D WLCSP and Si-based technologies.

Keywords: 3-D WLCSP, millimeter-wave applications, flip-chip, integration, assembly

1. Introduction

The firstly commercialized millimeter-wave application was the automotive radar, which appeared nearly 10 years ago, for driving safety support. The market size has been growing year by year and is expected to reach a level of around five million units per year in 2016. With the progress in popularity, the radar has been expected to spread even to general cars, therefore, development of low-cost and mass-productive technology for related components has become vital. In this situation, mass-productive SiGe hetero-junction bipolar transistor (HBT)^{(1), (2)} and complementary metal oxide semiconductor (CMOS)⁽³⁾⁻⁽⁵⁾ technologies have been competing with GaAs PHEMT technology. However, the discussion on "Si or GaAs" has not been settled because the radar unit is installed peculiarly near the engine room. Si and GaAs devices have been sharing the market recently. In addition, the market still requests flexible and speedy production methodologies to meet a marginal production volume per a type of radar. Sumitomo Electric Device Innovations, Inc. (SEDI) and Sumitomo Electric Industries, Ltd. have launched a novel wafer-level chip size package (WLCSP) technology⁽⁶⁾⁻⁽⁸⁾ by innovatively modifying three-dimensional (3-D) GaAs monolithic microwave integrated circuit (MMIC) technology. This 3-D WLCSP MMIC technology actualizes reliable flip-chip assembly on a printed circuit board (PCB) via tiny solder balls arranged on the surface pads and ground metal of MMIC, where neither package, wire bonding, nor tuning are necessary and a 3-D high integration is provided. Therefore, the GaAs 3-D WLCSP is a promising technology to meet the requirements for both simple assembly and mass production. These advantages have already been adapted to point-to-point communication MMICs between 13 GHz and 38 GHz. Various MMICs in the range of between microwave and millimeter-wave can be produced in the same form and design manners, resulting in easier development of 76 GHz/79 GHz-band automotive radar MMICs and 80 GHz-band (E-band) MMICs.

This paper introduces our research and development on millimeter-wave devices using the 3-D WLCSP MMIC

technology. Firstly, commercialized millimeter-wave radar modules will be described. Secondly, the structure and the features of the low-cost and mass-production basis 3-D WLCSP will be explained. Thirdly, various functional circuit designs with the 3-D WLCSP MMIC for the millimeter-wave radar and the E-band communication devices will be illustratively introduced. Advantages and benefits of our technology against other technologies will be additionally discussed.

2. Current Devices for Millimeter-Wave Radar

The millimeter-wave automotive radar instantly measures the distance between automobiles, where the frequency modulated continuous wave (FMCW) method is the main stream. A continuous wave in a saw-tooth-shaped frequency modulation is radiated forward and backward of an automobile to detect the reflected waves from the foregoing and following automobiles as beat signal. With the beat frequency f_r , the distance can be calculated. **Figure 1**

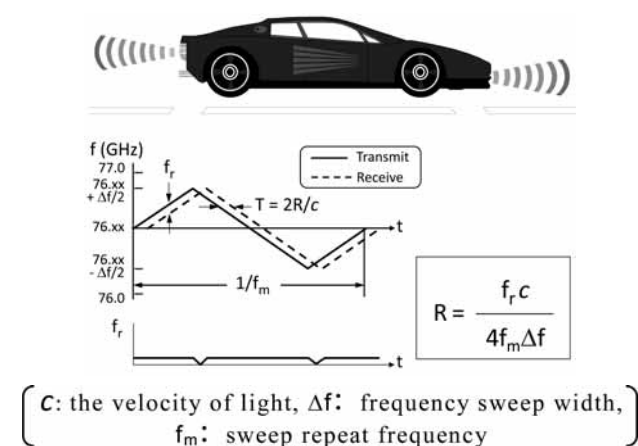


Fig. 1. Theory of FMCW radar

illustrates the theory and distance (R) formula.

Currently, the radiation frequency is limited between 76 GHz and 77 GHz (a 4 GHz bandwidth system centered at 79 GHz is planned to be used in the near future). In addition, there are strong demands for the frequency modulation to be highly linear and as low as possible in the phase noise level. In the case that the distance changes momentarily, f_r shifts occur and the wave form in Fig. 1 moves up and down due to the Doppler effect. The distance at a moment is calculated as a half the sum of neighboring f_r levels. The Doppler frequency is a half the difference of them.

The radar unit is installed behind the front emblem to radiate the modulated millimeter-wave signal forward. A millimeter wave goes through thin plating easily with little loss. This place is near the engine room and the radar unit is likely to become very hot. It also needs to start up instantly even in very cold environments. Therefore, the operation must be guaranteed in a wide temperature range of between -40°C and $+140^{\circ}\text{C}$.

The radar unit is required to be smaller and lighter due to the critical limits to installation and weight. To satisfy these requirements, the MMIC technology has been positively incorporated. The technology is also a key driver for mass production and cost reduction. The automotive radars are currently being developed to be installed in general cars, while previous radars were commercialized for luxury cars from 2000 to 2004. In this situation, MMICs became a more attractive and important device for radar applications. This caused an inevitable competition among GaAs PHEMT, SiGe, and CMOS devices.

Many radar units employ the configuration shown in Fig. 2. The FMCW voltage controlled oscillator (VCO) output is frequency multiplied to the 76 GHz-band signal by x multiplier (MLT), and the signal is amplified in the level up to greater than 10 dBm. A portion of the power is fed to a frequency converter (MIX) through a local oscillator amplifier (LOA) to generate the beat signal in Fig. 1. There are three issues of concern. The first one is to suppress the phase noise¹ of the VCO. The near-carrier phase noise (due to the $1/f$ noise) appears in the same frequency range as the beat signal. The second issue is the $1/f$ noise in the MIX itself, which can be measured as a noise figure² of the MIX at beat frequencies. These $1/f$ noises in the beat frequency range possibly degrade the detection accuracy. The

third one is to meet requirements to set the radar sensitivity high enough. The sensitivity is defined for the total transmit-receive path, and is evaluated with a figure of merit (FOM) $P_o G_c / N$, where P_o is the 76 GHz-band output power level, G_c the receiver conversion gain, and N the receiver noise figure. The FOM is essential to set the maximum detectable distance, and should be greater than a target value.

Furthermore, some different receiver configurations exist because there are several methods for radar scan with antenna(s). A millimeter-wave goes straight forward, while roads generally curve. Hence, the millimeter-wave beam must be scanned within a designated angle so as to always catch front and behind automobiles. Generally beam scan systems use electronic scan or mechanical scan. The electronic scan system needs several sets of antennas and receivers, and the mechanical scan a receiver and a mechanical scan antenna. It depends on the radar unit provider as to which system is selected.

The automotive radar components produced by SEDI are shown in Fig. 3. The component on the left is a 76 GHz-band transceiver module. A transceiver MMIC die is in a special design with use of gold pillars, and is flip-chip assembled in the thermal-press fashion on the backside of a ceramic substrate and hermetic shielded with a metal cap⁽⁹⁾. The component in the center is a hermetic-shield packaged 38 GHz-band VCO with a frequency quadrupler MMIC inside⁽¹⁰⁾. With the expansion of the radar market, the 9.5 GHz-band VCO was made in a single-chip and separately plastic-mold packaged, while the quadrupler was newly integrated in the transceiver die, resulting in lower cost. Unfortunately, these need additional small tunings.

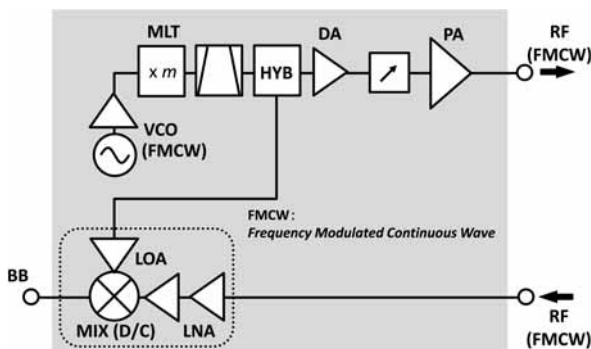
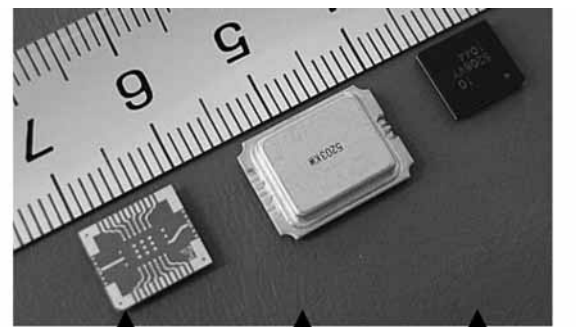


Fig. 2. A basic configuration of millimeter-wave module for automotive radar unit



76 GHz-band Transceiver (TRX MMIC package is on the backside) 38 GHz-band VCO (9.5GHz VCO and X4 MMIC are inside) 9.5 GHz-band VCO (9.5GHz VCO MMIC is plastic-molded)

Fig. 3. SEDI products for millimeter-wave radar

3. 3-D WLCSP Technology

The 3-D WLCSP MMIC is a novel MMIC. Polyimide multi-layers are spin-coated on and over the surface of semiconductor wafer and the microwave/millimeter-wave circuitry is constructed among the multi-layer structure. Transistors (PHEMTs), capacitors, and resistors are formed

in and on the surface of GaAs substrate. Due to a ground metal covering the polyimide structure, the MMIC can be flip-chip assembled with very little degradation in performance^{(6), (11)}.

Figure 4 illustratively compares the 3-D WLCSP and conventional MMICs. The upper figure is for the conventional, and the lower is for the 3-D WLCSP. With the conventional one, high integration of circuitry is not easy because the GaAs substrate is used as the core medium of a transmission line. In addition, the bonding wires affect and degrade MMIC performance severely at millimeter-wave frequencies. Radiation from the wire, in some cases, makes the assembled MMIC unstable. Even when the wire length is the shortest, the variation in length and the inductance degrades the yield. For reflow soldering assembly, an interposer for surface mount is additionally necessary.

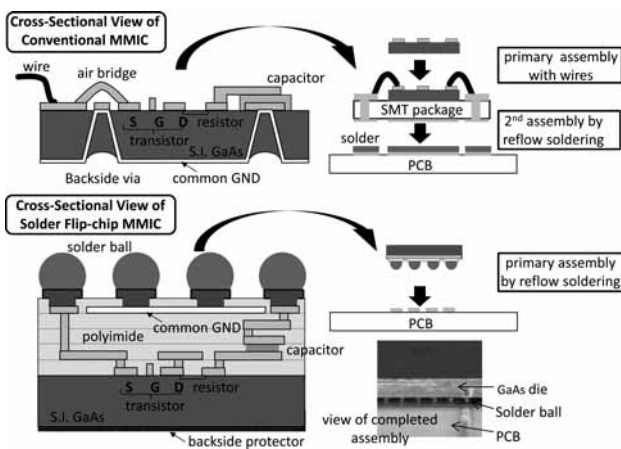


Fig. 4. Comparison between 3-D WLCSP and conventional MMIC technologies

The 3-D WLCSP MMIC can employ miniature transmission lines with a width of nearly $10\ \mu\text{m}$ and spacing between line segments of as narrow as $> 30\ \mu\text{m}$. Devices and line strips on different layers can be connected easily via tiny through holes. The transmission lines are characterized and specified in the design library on the premise that the multi-layer structure is covered with ground metal. The WLCSP MMIC is completed after signal I/O- and power supply-pads and grounding pads are formed in combination with barrier metal³, and then tiny solder balls are automatically put on the pads. This MMIC requires no packaging because each polyimide layer is treated so as to be humidity proof. This miniature transmission line and solder ball enable high-integration and flip-chip reflow soldering, resulting in a high-level mass production with no wiring. The production process is very simple as shown in **Fig. 5**. Through dicing a wafer with arrayed balls, many products are simultaneously produced.

Although this technology had been primarily developed and completed to commercialize devices for radio-link applications in several frequency bands between 13

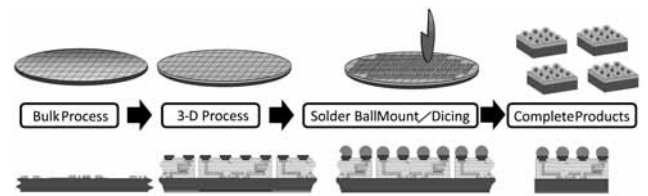


Fig. 5. Attractive production process of 3-D WLCSP MMIC

GHz and 42 GHz, its applicable high frequency edge reaches 100 GHz (see **Fig. 6**). As the 3-D WLCSP MMIC has a humidity proof property, no packaging is necessary. With these features, low cost and simple assembly is performed. Therefore, this WLCSP structure can be a mass-production platform in all the frequency ranges in **Fig. 6**.

frequency	4 GHz - 15 GHz	15 GHz - 40 GHz	40 GHz - 90 GHz
Conv. chip set *	plastic mold	ceramic	bare die
SEDI WLCSP	3-D WLCSP form only		

* The photos are from Hittite Microwave Corporation's website.

Fig. 6. Form comparison between 3-D WLCSP MMIC and conventional MMIC products

4. Design Methodologies on WLCSP

The 3-D WLCSP MMIC the surface of which is covered with ground metal provides miniature transmission lines as narrow as around $10\ \mu\text{m}$. On the other hand, an increase in the line loss due to the narrow line width possibly degrades circuit performance. Firstly, to guarantee higher gain, we improved PHEMT performance (gate width: $0.1\ \mu\text{m}$, f_r : 85 GHz, f_{max} : 230 GHz, NF_{min} at 12 GHz: 0.5dB), and furthermore, incorporated a novel high-gain amplifier topology. Success of a MMIC design platform depends on amplifier performance. Hereafter, design examples of amplifier, frequency multiplier, frequency converter, and oscillator will be described individually.

A. Amplifier

Newly employed high-gain amplifier topology and the performance are shown in **Fig. 7**. This is one of current reuse amplifiers in which the drain bias current provided to the second PHEMT is also fed to the first one via the source of the second PHEMT⁽¹²⁾. Each gate bias voltage is determined by resistor R_s . In this topology called Dual-HEMT, the circuitry required for DC bias is very simple and miniature lines can be effectively used, resulting in significant size reduction of the amplifier. A gain of as high as 12 dB can be achieved even at 76 GHz-band. This high gain performance is produced by a high impedance coupling between PHEMTs. It is because stray capacitances of the PHEMTs are canceled in the configuration enclosed with dotted line. The gain of this portion, S_{21}^{DUAL} , is expressed

as follows, where Y_{ds} is the drain-source capacitive admittance of PHEMT. By adjusting the absolute of denominator to be $1/2$ with suitable θ and Y_{RL} , $|S_{21}^{DUAL}|$ becomes $(2g_m Z_0)^2$, while the gain of single common-source (CSF) PHEMT is $2g_m Z_0$. The current reuse amplifier's gain is twice in dB of the CSF amplifier's. Some other conditions possibly provide higher gains. Furthermore, the matching circuitry loss is halved compared with CSF two-stage amplifier. Hence, the topology in Fig. 7 is the most suitable one in the 3-D WLCSP utilizing narrow transmission lines. Figure 8 shows a three-stage current reuse amplifier, originally called Triple-HEMT, designed as an E-band amplifier. This gain is greater than 14 dB in the frequency range of from 55 GHz to 92 GHz, as shown in Fig. 8. The circuit size is 0.8 mm x 0.5 mm.

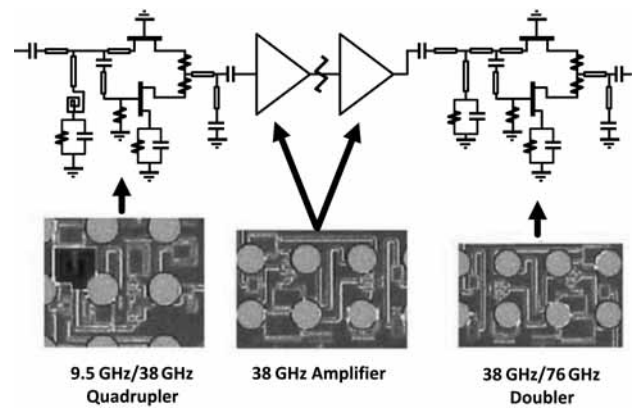


Fig. 9. The circuit configuration of a 9.5 GHz/76 GHz multiplier (Each circuit area is less than 0.25 mm²)

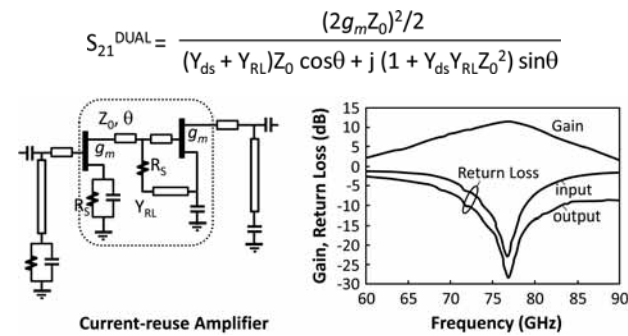


Fig. 7. Circuit configuration and performance of a 76 GHz-band current-reuse amplifier

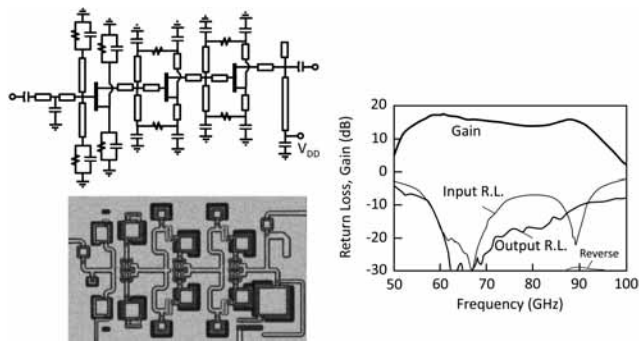


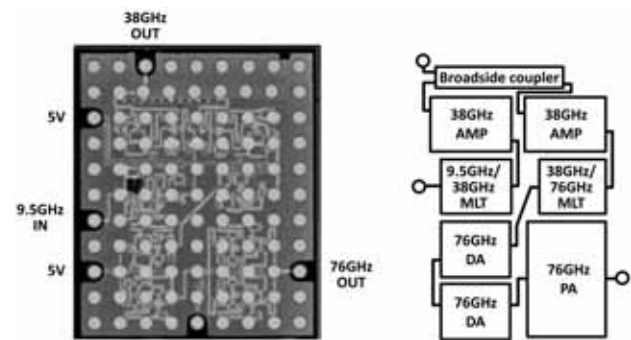
Fig. 8. An E-band high gain amplifier in triple-HEMT topology

B. Frequency Multiplier

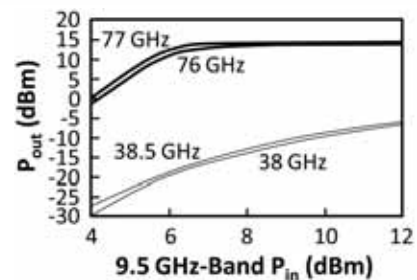
In the millimeter-wave radar, a 9.5 GHz-band signal is converted to 76 GHz-band one by frequency multipliers. The frequency multipliers in Fig. 9 are realized in a small size by combining PHEMTs in different common-ground systems^{(13) *4}. As the signal phase transmitted through common-gate PHEMT is ahead by π compared to that through common-source PHEMT, only even harmonics are output. According to this system, a 9.5 GHz/38 GHz quadrupler and 38 GHz/76 GHz doubler are realized, where 38 GHz amplifiers in saturation operation are inserted between the multipliers to maximize and stabilize the 76 GHz-band out-

put power level. A 76 GHz-band amplifier chain following the x8 multiplier achieves a desired power level and completes a radar transmitter. In the photos, the circles arranged in array are metal pads for installing solder balls.

The die photograph and performance of a transmitter MMIC with the multiplier is shown in Fig. 10. The die size is 1.5 mm x 2.0 mm (the intrinsic area is 1.1 mm x 1.7 mm). At a 9.5 GHz-band input power level of 6 dBm, a 76 GHz-band output power level reaches 14 dBm. This transmitter keeps the output power level stable, in the wide temperature range, at input power levels higher than 10 dBm. The dissipation power is 650 mW.



(a) TX MMIC and its block diagram



(b) Measured output power characteristics

Fig. 10. The 76 GHz-band transmitter and its power performance

The E-band transmitter under development needs a $\times 3$ multiplier (tripler). This system requirement is given to suppress undesired products into the communication band. Here, it is really important to generate the third harmonics effectively for the E-band local oscillator (LO), and also suppress the even harmonics. A unique tripler circuit topology and the performance of the tripler with additional output amplifier are shown in **Fig. 11**. The maximum frequency range required for the E-band LO is between 60 GHz and 96 GHz. The input signal source frequency is between 20 GHz and 32 GHz. The second and the fourth harmonic frequencies are between 40 GHz and 64 GHz and between 80 GHz and 128 GHz respectively. These even harmonic frequency ranges partially overlap the E-band LO range. Additionally, the second harmonic level is nearly 10 dB higher than that of the desired third one. Therefore, the circuit topology is structured to combine the second harmonic outputs out of phase. The third harmonics outputs are combined orthogonally. The tripler shown in the photo is 0.8 mm x 0.8 mm in size.

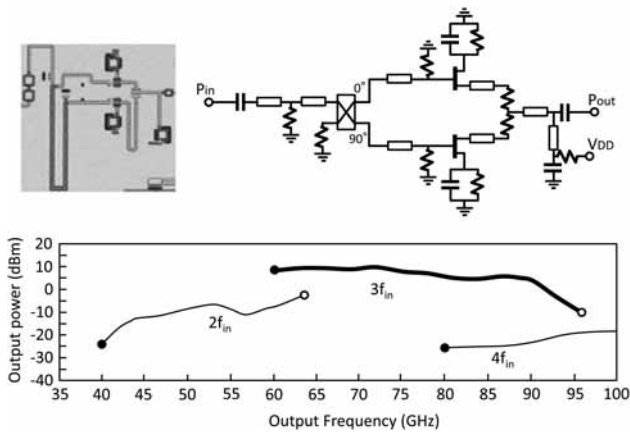


Fig. 11. The circuit configuration employed for tripler and its performance with additional output amplifier

C. Frequency Converter

While the receiver configuration for millimeter-wave radar depends on its beam scan system, a mixer for frequency conversion is necessary at least. The mixer needs to be small in size, as the LO multiplier is for compact receivers, and also to provide linearity for the 76 GHz-band input, LO-to-RF leakage suppression, and singular IF output port. These issues can be simultaneously solved with the mixer configuration in **Fig. 12**. A pair of PHEMTs is operated with no DC bias and excited by the gate LO voltage. This is a resistive mixer⁵ that exhibits high linearity. The coupler is a broadside coupler⁶ that is compactly constructed in the multi-layer structure with -3 dB and 0°/90° coupling. It is the same as in **Fig. 11**. Because of the thin multi-layer structure with the surface ground metal on it, it is necessary to increase Z_{even} for realizing $Z_0 = (Z_{\text{even}} \cdot Z_{\text{odd}})^{1/2}$. The slit in the right figure is the solution. The slit width is merely 20 μm , hence, the coupler is very compact. The divided LO signals appear out of phase, through the PHEMTs, on the RF port

and they cancel each other. The baseband signals as the beat of RF and LO signals are generated in the PHEMTs and output in phase. **Figure 13** presents the photo and performance of this mixer. The occupation area is roughly 0.15 mm², and the 1-dB gain compression point $P_{1\text{dB}}$ that indicates linearity is at an input power level of 5 dBm.

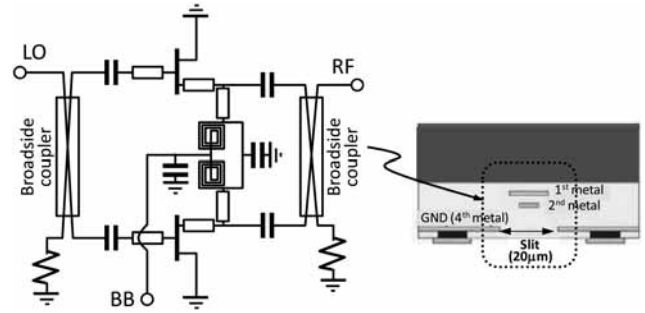


Fig. 12. Mixer configuration with broadside couplers

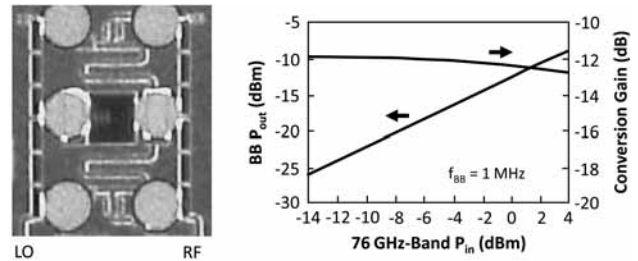


Fig. 13. An implemented mixer MMIC and the performance

A low noise amplifier is connected to the mixer RF port and a chain of a multiplier and an amplifier is connected to the mixer LO port. In the case that a 38 GHz-band signal is fed from the transmitter to the mixer, the multiplier is a doubler. The use of the 38 GHz delivery from transmitter (TX) to receiver (RX) avoids undesired oscillation or instability when TX and RX dies are separated. With such a chipset we can flexibly design receivers. An example of flexible receiver design with two receiving ports is shown in **Fig. 14**. Its performance was conversion gain of 10 dB and input $P_{1\text{dB}}$ -12 dBm. The noise figure increased below 1MHz beat frequency due to the $1/f$ noise of the PHEMT. This should be improved.

The E-band radio-link RX/TX mixers are strictly required to perform suppression of both LO-to-RF leakage and image response. The image response must be suppressed so as not to degrade the quality of IF output signal. This operation is possible by combining a pair of mixers in **Fig. 12** orthogonally for the LO ports and in phase for the RF ports, or vice versa. However, for higher LO-to-RF leakage suppression, the unit mixer topology needs to be changed and improved. Additionally, for better linearity with lower 3rd inter-modulation, a linear low noise amplifier should be designed. These requirements are also impor-

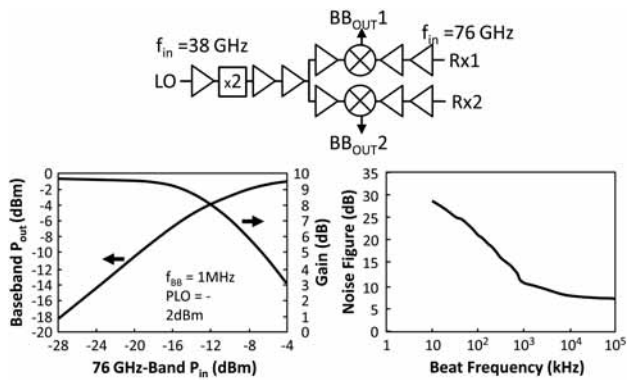


Fig. 14. An example of 76 GHz-band receiver with two input ports

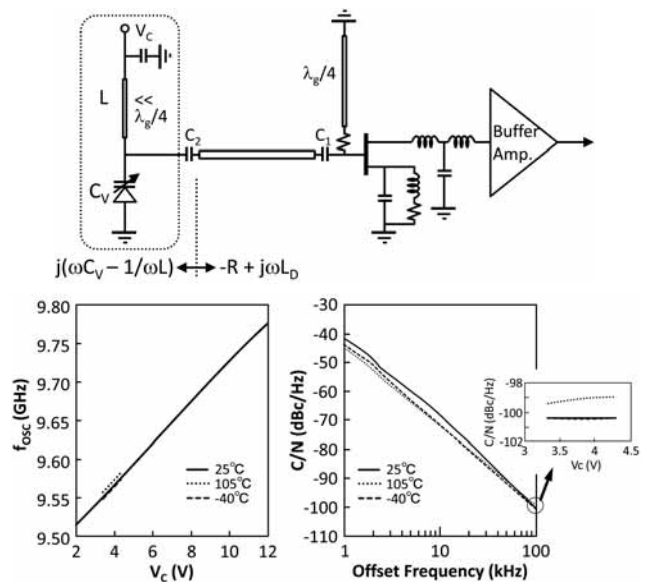


Fig. 16. The configuration and performance of linear VCO

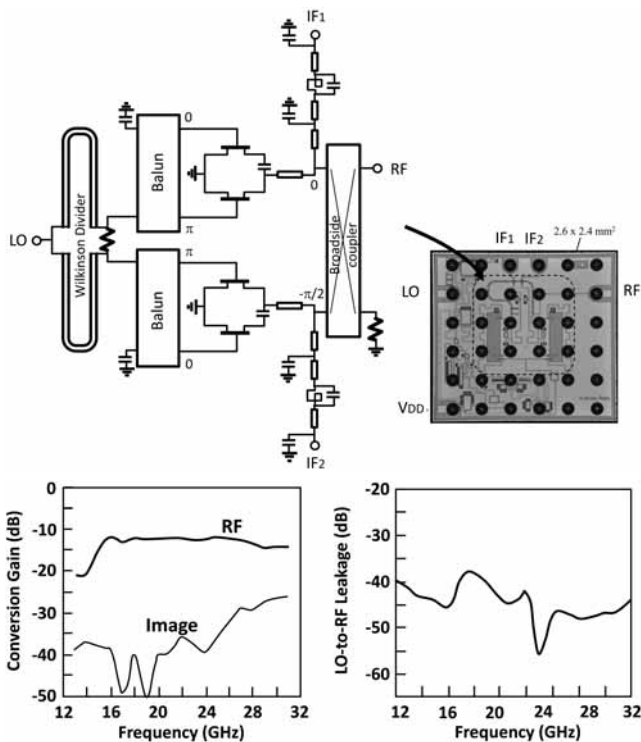


Fig. 15. An example of 3-D WLCSP radio-link mixer

tant when designing other radio-link mixers. The scheme of a radio-link 18-23 GHz mixer and its performance are demonstrated in Fig. 15. The mixer incorporates a novel balun⁷ with excellent out-of-phase power dividing performance. The LO-to-RF leakage suppression is >20 dB greater than that of the mixer in Fig. 12. In the category of 3-D WLCSP, this topology can be applied to the E-band with little difficulty.

D. Oscillator

Oscillators based on the 3-D WLCSP are under development. The phase noise performance has not reached the required level. The 9.5 GHz-band VCO shown in Fig. 3 or other commercialized VCO modules are the candidates for use now. The basic configuration of such VCOs is shown in Fig. 16⁽¹⁰⁾. A linear frequency tuning scheme is illustrated

in the area enclosed with dotted line. The ideal C-V characteristic of the varactor is $C \propto V^{-2}$ ⁸, while the best commercial varactor exhibits $C \propto V^{-3/4}$. To make up the available varactor characteristic similar to the ideal one, an inductive line is connected to a varactor in parallel. This works to shift the $C \propto V^{-3/4}$ curve downward, resulting in a total C-V characteristic overlapping the ideal one. This modified variable capacitance circuit is attached on one side of the resonator. A $>1/4$ wavelength line with small capacitances on both sides of it is used to achieve the VCO's Q factor as high as 30. The achieved phase noise level was -100 dBc/Hz at 100 kHz offset. This is low enough for practical radar applications, and simultaneously the frequency tuning is performed linearly.

On the other hand, PLL VCOs with phase-locked loop

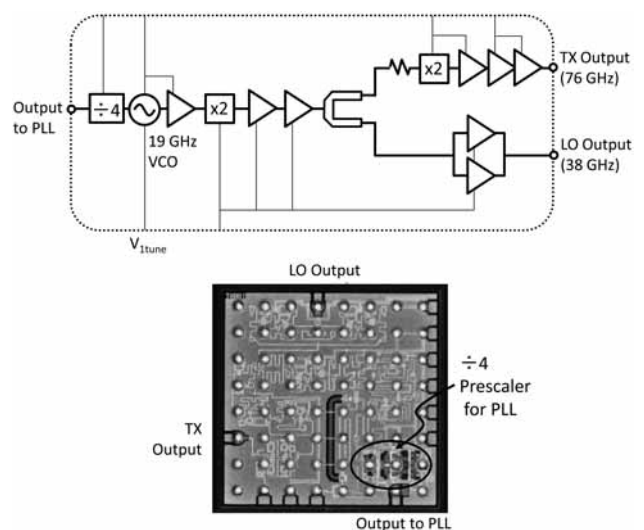


Fig. 17. A 3-D WLCSP transceiver with a 1/4 prescaler

are often employed in other companies' SiGe HBT products. Its feature is that the VCO and prescaler are integrated on a die. However, external crystal oscillator or digital oscillator as phase reference and other accessories are necessary. This method is possibly a candidate when no stand-alone low phase noise VCO will be developed with the 3-D WLCSP. An example of radar transceiver that integrates a prescaler is shown in Fig. 17.

5. Superiorities to Other Technologies

The combination of GaAs PHEMT and 3-D WLCSP is superior to other devices and technologies.

Firstly, the cost of the GaAs PHEMT process is lower than that of SiGe HBT, and lower than that of millimeter-wave CMOS established with an ultra-short gate length (< 100 nm). As for the mask set with which the fabrication is proceeded step by step, the cost for GaAs PHEMT is the lowest. Hence, the mask set can be revised relatively frequently. The cost can be roughly estimated 1/10 or less than that of other processes. The automotive radar market is too small for the ultra-short gate CMOS, the mask set of which costs around 1 million dollars. It is difficult to maintain an exclusive process line for advanced CMOS radar devices. The automotive radar and other millimeter-wave devices are currently niche products in the CMOS field. Furthermore, it is often pointed out that SiGe HBT application is limited and will exhibit little popularity in the future. This device is a family of bipolar transistors and exhibits very low $1/f$ noise characteristics, therefore, suitable for VCO. However, it is unsuitable as a low noise amplifier or power amplifier. Contrarily to such Si family devices, the GaAs PHEMT, which has a wide range of application fields, is considered to be suitable for automotive radar development.

Secondly, PHEMT exhibits higher output power than Si devices and is reliable even in the saturated operation. The thermal dependence of the output power level is suppressed within ± 1 dB. On the other hand, SiGe HBT cannot be operated in the saturation mode because it is driven by the base current. Hence, a SiGe HBT amplifier must be controlled in gain so as not to reach the saturation level, where the gain easily varies with temperature, and so, feedback of a temperature sensor output to the amplifier is necessary to set the amplifier gain stable. In other words, the temperature-sensitive SiGe HBT's g_m needs to be well controlled for stable and high output power. In this regard, the GaAs PHEMT is superior in power performance to the SiGe HBT. The short-gate CMOS exhibits severe drain voltage drop along with a gate-length shrink. It is roughly 1V for CMOS in millimeter-wave application. Although stacked CMOS topologies have been under research, no practical outcome has been reported yet.

Thirdly, the 3-D WLCSP is superior to other structures in assembly and cost, and the technology has been positively applied to the 13/15 GHz-, 18/23 GHz-, 24/30 GHz-, 32 GHz-, and 38 GHz-radio-link commercial products. The millimeter-wave MMICs are, simply to say, recognized as a family. As the die assembly on to PCB is performed via solder balls as small as nearly 150 μm in diameter, little perform-

ance degradation is observed even at millimeter-waves. This technology is not available for SiGe HBT and CMOS products based on conductive Si substrate. The Si MMICs are assembled in a package or on PCB with fine gold- or aluminum-wires. At the present time, the fact there is no low-cost millimeter-wave package with practically good performance obliges bare die assembly on PCB with bonding wires. The bonding wire exhibits an inductance, effect of which is fairly large at millimeter-waves even with a wire as short as 100 μm . As a result, the performance repeatability becomes worse naturally in mass-production.

Performance of a flip-chip assembled 3-D WLCSP amplifier (solid line) and its performance obtained by probing the bare die (dotted line) are compared in Fig. 18 (a). Performance of a wire assembled conventional 2-D MMIC amplifier (solid line) and its performance obtained by probing the bare die (dotted line) are compared in Fig. 18 (b), where the wire is stretched to 200 μm in length. All of them are measured performances. Comparing the bare die performances, the 2-D MMIC amplifier is better than the 3-D WLCSP one in the noise performance. However, when the 2-D one is wire assembled, the difference is suppressed. The gain and return loss characteristics are more stable for the 3-D WLCSP than for the 2-D MMIC. In any case, the wire length of 200 μm is not a practical condition in mass-production assembly. From a reliability point of view, the wiring must be performed with an enough loop. This further degrades the performance of assembled 2-D MMIC amplifier. A 300- μm -long loop wire provides a noise figure of around 6 dB. Generally beyond 40 GHz, unpredictable performance variations among products are observed. These variations are out of recovery and also a critical problem. As a conclusion, the 3-D WLCSP performance is superior after assembled and suitable for mass-production.

6. E-band Transceiver

An E-band transmitter (TX) and receiver (RX) were made for trial after preparing the 3-D WLCSP components. The breadboards incorporate an LNA in Fig. 18 (a), a couple of triplers in Fig. 11, a set of mixers (U/C, D/C) the core portion of which is similar to that in Fig. 12, and three power amplifiers with a large gate width. Additionally, a microstrip line-to-waveguide (WG) transition was realized on PCB. A block diagram and photos of the fabricated transceiver breadboard models are shown in Fig. 19. The design strategy is that each functional MMIC covers the entire E-band (71 – 76 GHz, 81 – 86 GHz). The broadband design and die-size shrink were achieved by effectively utilizing the 3-D miniature transmission lines. The photos are actually proving that transmitter and receiver can be produced easily through flip-chip and reflow soldering procedure. The area occupied by the millimeter-wave TX and RX is as small as a 500-yen coin. As seen here, the very small and simple realization of millimeter-wave equipment is an excellent feature of the 3-D WLCSP. Some measured performance of the receiver is shown in Fig. 20.

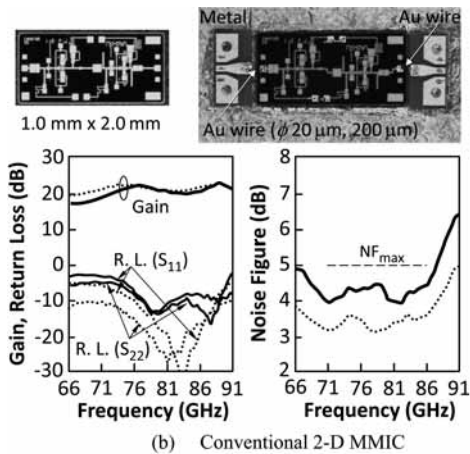
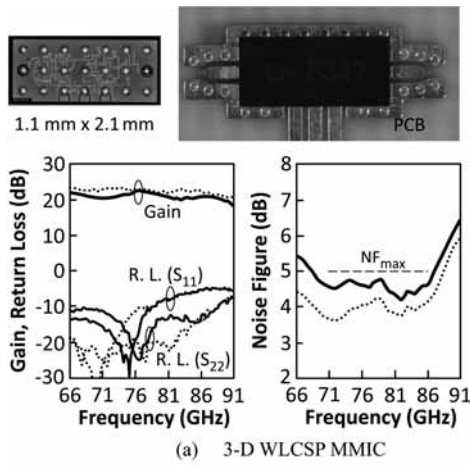


Fig. 18. Differences between 3-D WLCSP and conventional 2-D MMICs

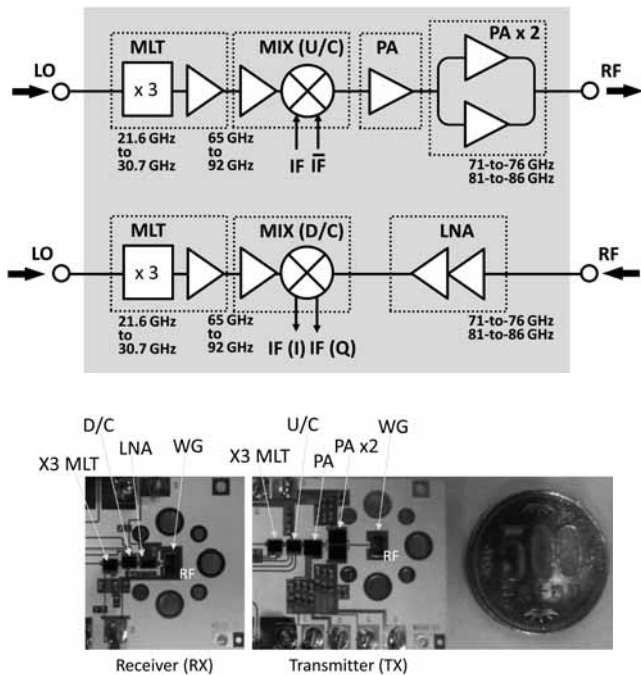


Fig. 19. E-band RX and TX breadboards

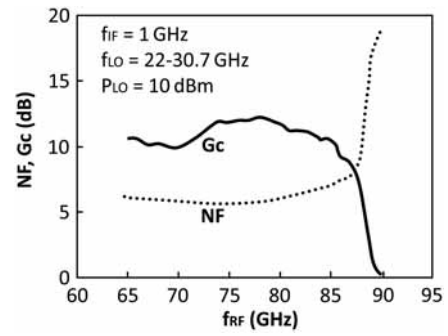


Fig. 20. Performance example of RX board

7. Conclusion

Application of GaAs devices to a millimeter-wave automotive radar and E-band transmitter as well as SEDI's and Sumitomo Electric's original design platform named 3-D WLCSP MMIC technology were introduced. The 3-D WLCSP MMIC has already been applied to the point-to-point radio link up to 38 GHz. This technology is valuable even at millimeter-waves. Microwave and millimeter-wave devices can be designed and produced in a simple manner and in a consistent form with solder balls suitable for flip-chip assembly. This outstanding feature possibly offers mass-production solutions to both the growing markets. We will continuously improve this technology to meet the market requirements.

Technical Terms

- *1 Phase noise: There exist noises inside a transistor, one of which is $1/f$ noise inversely proportional to frequency at low frequencies, and the other is white (thermal) noise. The $1/f$ noise, which is also called flicker noise, occurs due to electron flicker. These noises equivalently give a narrow-band FM modulation to the oscillation signal, and then produce oscillation spectral with skirts on both sides of the carrier frequency. The level at each skirt frequency is called phase noise and measured with unit dBc/Hz.
- *2 Noise figure: Defined as ratio of output S/N to input S/N. Noise figure $F = (S/N)_{IN} / (S/N)_{OUT}$.
- *3 Barrier metal: The solder ball attached directly on gold pad corrodes the gold, resulting in reliability problem. Hence, it is necessary to cover the pad with some metal which prevents corrosion. This metal is called barrier metal.
- *4 Common ground system: PHEMT has three electrodes called gate, source, and drain. The device's transmission performance changes significantly by the electrode chosen for common ground. When the gate is chosen for it, the angle of S_{21} is 0 and the input impedance at source is $1/g_m$. When the source is chosen for common ground, the angle of S_{21} is π and the input impedance at gate is high. With these PHEMTs combined in parallel, an input signal transmits through the paths out of phase to each other and in the same amplitude.

- *5 Resistive mixer: This mixer utilizes the I-V characteristics of PHEMT at $V_{DS} = 0$ V, where I-V slope grade can be changed between low and high. This is equal to switching the PHEMT's channel to give a non-linearity to the channel conductance. The non-linearity is expressed as $g_{DS} = \sum_{n=-\infty}^{\infty} g_n e^{jn\omega_{LO}}$, (n : integer). By multiplying g_{DS} with an RF or IF signal applied to the PHEMT drain, down- and up-conversion is performed. This operation keeps the non-linearity (g_n) constant until the applied signal level reaches the knee voltage V_k , therefore, a highly linear frequency conversion can be performed.
- *6 Broadside coupler: Electro-magnetic coupling between two line segments increases as the spacing decreases. However, the coupling on a plane is limited (< -6 dB). This is because the spacing for higher coupling becomes narrower than MMIC process limit. On the other hand, the capacitance between two lines significantly increases by stacking them, achieving tight coupling. This structure called broadside coupler is suitable for the 3-D WLCSP with thin multi-layers.
- *7 Balun: Balun is a circuit component which divides an input signal to two out-of-phase signals. Microwave engineers usually use this term. The balun shown in Fig. 15 utilizes a 90° coupler the through and isolation ports of which are connected through a half wavelength line and the coupling port of which is grounded.
- *8 $C \propto V^2$: Oscillation frequency is given by $f_{osc} = 1 / (2\pi \sqrt{LC})$. When L is constant and $C \propto V^2$, f_{osc} is proportional to $V / (2\pi \sqrt{L})$. This means that oscillation frequencies proportional to V is obtained when $C \propto V^2$.

References

- (1) H. P. Forstner et al., "A 77GHz 4-channel automotive radar transceiver in SiGe," in IEEE Radio Frequency Integrated Circuits Symposium Dig., Atlanta, pp. 233-236 (June 2008)
- (2) L. Wang et al., "A single-ended fully integrated SiGe 77/79GHz receiver for automotive radar," IEEE J. Solid-State Circuits, vol. 43, no. 9, pp. 388-391 (Sep. 2006)
- (3) Y. Kawano et al., "A 77GHz transceiver in 90nm CMOS," in IEEE ISSCC Dig., pp. 310-312 (2009)
- (4) T. Mitomo et al., "A 77GHz 90nm CMOS transceiver for FMCW radar application," in IEEE Symposium on VLSI Circuits Dig., pp. 246-247 (2009)
- (5) V. H. Le et al., "A CMOS 77-GHz receiver front-end for automotive radar," IEEE Trans. Microwave Theory Tech., vol. 61, no. 10, pp. 3783-3791 (Oct. 2013)
- (6) M. Imagawa et al., "Cost effective Wafer-Level Chip Size Package technology and application for high speed wireless communications," in the 39th European Microwave Conf. Proc., Rome, pp. 49-52 (Sept. 2009)
- (7) K. Tsukashima et al., "Cost effective Wafer Level Chip Size Package technology and application to the next generation automotive radar," in the 40th European Microwave Conf. proc., Paris, pp. 280-283 (Sept. 2010)
- (8) K. Tsukashima et al., "E-band receiver and transmitter modules with simply reflow-soldered 3-D WLCSP MMIC's," in the 8th European microwave Integrated Circuits Conf. Proc., Manchester, pp. 588-591 (Oct. 2013)
- (9) Y. Ohashi et al., "76 GHz flip-chip MMIC's in through-hole package," in the 28th European Microwave Conf. Proc., Amsterdam, pp. 433-438 (Oct. 1998)

- (10) T. Tokumitsu et al., "Very linear and low-noise Ka/Ku-band voltage controlled oscillator," IEICE Trans. Electron., vol. E85-C, no. 12, pp. 2008-2014 (Dec. 2002)
- (11) T. Tokumitsu, "Three-dimensional MMIC and its evolution to WLCSP technology," SEI Technical Review, no. 72, pp. 35-42 (April 2011)
- (12) Y. Mimino, et al., "High gain-density K-band P-HEMT LNA MMIC for LMDS and satellite communication," in 2000 IEEE International Microwave Symposium Dig., Boston, pp. 17-20 (June 2000)
- (13) Y. Mimino et al., "A 60 GHz millimeter-wave MMIC chipset for broadband wireless access system front-end," in 2002 IEEE International Microwave Symposium Dig., Seattle, pp. 1721-1724 (June 2002)

Contributors (The lead author is indicated by an asterisk (*).)

T. TOKUMITSU*

- Senior Specialist
Ph. D.
Senior Chief Engineer, Transmission
Devices R&D Laboratories
IEEE Fellow



M. KUBOTA

- Group Manager, Transmission Devices
R&D Laboratories



K. SAKAI

- Manager, Electronic Device Department,
Sumitomo Electric Device Innovations,
Inc.



T. KAWAI

- General Manager, Electronic Device
Department, Sumitomo Electric Device
Innovations, Inc.

